Scaling of Electron and Ion Transport in the High-Power Spherical Torus NSTX

S. M. Kaye,[1] R. E. Bell,[1] D. Gates,[1] B. P. LeBlanc,[1] F. M. Levinton,[2] J. E. Menard,[1] D. Mueller,[1] G. Rewoldt,[1] S. A. Sabbagh,[3] W. Wang,[1] and H. Yuh[2]

[1]*Princeton Plasma Physics Laboratory, Princeton University, Princeton, New Jersey 08543, USA*
[2]*Nova Photonics Inc., Princeton, 08540 New Jersey, USA*
[3]*Department of Applied Physics, Columbia University, New York, 10027 New York, USA*

(Received 21 November 2006; published 26 April 2007)

Dedicated H-mode parameter scans in the high-power National Spherical Torus Experiment have been used to establish the confinement scaling and underlying transport trends at low aspect ratio ($R/a \simeq 1.3$). These scans indicate a strong dependence of the global and thermal energy confinement times on the toroidal field, $B_T^{0.9}$, while their dependence on plasma current is weaker, $I_p^{0.4}$. Local transport analysis indicates that the electrons control the B_T scaling, whereas the ions control the I_p scaling, with χ_i outside $r/a = 0.5$ at the neoclassical level.

DOI: 10.1103/PhysRevLett.98.175002 PACS numbers: 52.55.Fa

Energy confinement scaling experiments to identify the underlying H-mode transport trends at low aspect ratio have been carried out on the National Spherical Torus Experiment (NSTX). NSTX, with a major radius $R = 0.85$ m and minor radius $a = 0.65$ m, operates at a low aspect ratio ($R/a \simeq 1.3$) using up to 7 MW of deuterium neutral beam injection into deuterium plasmas [1,2]. Because of the high primary beam energy, 90 keV, the neutral beams heat electrons preferentially over ions in NSTX by about a 2:1 ratio. NSTX also operates at low toroidal magnetic field, $B_T = 0.3$ to 0.55 T, plasma currents up to 1.5 MA, elongations κ up to 2.8 and triangularities δ up to 0.8 in diverted H-mode plasmas.

Early projections of ion transport in NSTX suggested that the long wavelength turbulence driving the anomalous ion transport should be stabilized by geometrical and $E \times B$ shear effects, and thus the ion transport should approach the neoclassical level [3]. This raised the possibility that the confinement trends might be different from those observed at higher aspect ratio. Early confinement results from NSTX did indeed indicate some differences between low and high aspect ratio, most notably in the toroidal field and plasma current scalings [4]; however, these results were hampered by colinearities among the so-called independent engineering variables. We present here first time results from dedicated confinement scans at high power in NSTX in which the B_T and I_p scalings have been isolated from changes in other parameters. While the B_T scaling is found to be strong, the I_p scaling is found to be weaker, in contrast to what is observed at higher aspect ratio as embodied in the ITER98PB(y,2) scaling [5]. Local transport analyses indicate that while electrons primarily control the B_T scaling, the ion transport controls the I_p scaling. In both the B_T and I_p scans, the ion transport outside of $r/a = 0.5$ is at the neoclassical level. Thus, NSTX provides an excellent laboratory for identifying and studying the processes causing anomalous electron transport.

In both the I_p and B_T scans, the plasmas were lower single null divertor discharges with $\kappa = 2.1$, $\delta = 0.6$ and with constant injected power of 4 MW. A B_T scan from 0.35 to 0.55 T was performed at two currents, $I_p = 0.7$ and 0.9 MA, while an I_p scan was performed at $B_T = 0.55$ T. All discharges were well into the H-mode phase at the time of interest, with small amplitude, type V [6], edge localized mode (ELM) activity. The ELMs in both scans were similar, exhibiting D_α fluctuations of comparable amplitude from 0.1 to 1.0 kHz. The plasmas in these scans were below the instability limit of approximately $\beta_N = 5.5\%$-T/MA, calculated for pressure-driven instabilities stabilized by the nearby conducting wall [7]. The Z_{eff} profiles for both scans, inferred from the carbon density profile measurements, were inverted, with values from 1.5 to 2.5 in the center of the plasma, increasing with decreasing current, and 3.0 near $r/a = 0.8$. The central Alfvén Mach number for all discharges varied from 0.17 to 0.26.

The plasma densities and density profiles in the discharges for each scan were similar at the times of interest, allowing both the B_T and I_p dependences of confinement to be isolated. In previous experiments, the variation in density was strongly coupled to that in both I_p and B_T, with correlation coefficients of 0.54 and 0.42, respectively. In the scans reported here, the coefficients were reduced to 0.16 and 0.19. Between-shots helium glow discharge cleaning with durations from 10 to 13 min was employed to maintain similar densities from discharge to discharge. Several discharges were run at each condition of each scan to verify reproducibility.

The variations of both the thermal and global confinement times are shown in Figs. 1(a) and 1(b) for the B_T scan at 0.7 MA and the I_p scan, respectively. The definition of the B_T used here is the applied toroidal magnetic field at the plasma geometric center. The confinement times are defined as $\tau = W/P_L$, where W represents either the thermal or thermal plus fast ion stored energy for the thermal

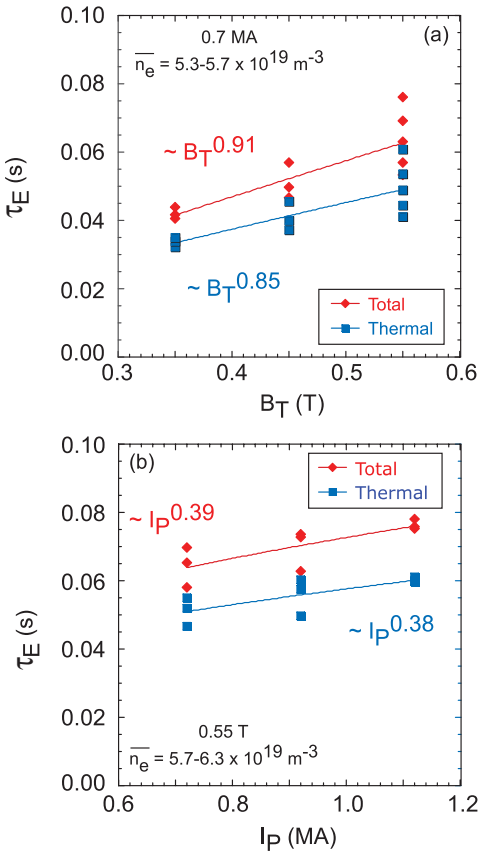

FIG. 1 (color). Thermal and global confinement time scalings as a function of (a) B_T and (b) I_p from dedicated scans at constant injected beam power, 4 MW, and density.

and global τ_E, respectively, and P_L is the total heating power less dW/dt and the fast ion losses due to shine thru, bad orbit, and charge exchange, which were between 13% and 20% of the injected power. The stored energy and losses are based both on measurements and calculations of classical neutral beam dynamics in the TRANSP code [8,9]. Figure 1(a) shows the B_T scaling to be strong, with $\tau_{E,\mathrm{th}} \sim B_T^{0.85\pm0.19}$ and $\tau_{E,G} \sim B_T^{0.91\pm0.19}$ for the thermal and global confinement times, respectively. This is a much stronger variation than is observed in conventional aspect ratio tokamaks, as reflected by the ITER98PB(y,2) scaling, [5] where $\tau_{E,\mathrm{th}} \sim B_T^{0.15}$. In the higher current (0.9 MA) scan, the B_T dependence was weaker, with both τ_E values varying as $B_T^{0.6}$, suggesting a possible dependence of the strength of this scaling on q. The dependence on plasma current [Fig. 1(b)] is weaker, with both the global and thermal τ_E going as $I_p^{0.4\pm0.13}$. In comparison, the I_p dependence for the ITER98PB(y,2) scaling is $I_p^{0.93}$. In both scans, the density range at the times of interest was narrow, $\leq$10% variation, and as was indicated above, the density profiles were well matched.

Local transport analysis has been carried out to determine whether it is the electron or ion channel, or both, that is responsible for the B_T and I_p confinement trends in NSTX. The transport analysis was carried out using the TRANSP code, which combines measured profile data with a Monte Carlo calculation of the neutral beam ion thermalization to determine particle and heat source and loss terms and to infer the transport coefficients for each of the species. The equilibria used in the TRANSP calculation were taken from LRDFIT equilibrium reconstructions, [7] with most reconstructions constrained by magnetic field pitch measurements from the 12-channel motional Stark effect diagnostic. The neutral beam ions were assumed to behave classically (i.e., no MHD-induced or other anomalous losses). Some of the discharges in this study did exhibit both low-amplitude low-n MHD activity as well as the fast ion driven Alfvén eigenmode (AE) activity, which could potentially lead to fast ion redistribution and/or loss. The levels of the AE modes, when present, were generally low as compared to activity levels that are known to cause significant loss or redistribution of fast particles. The sensitivity of the local transport coefficients to the assumption of classical slowing down was nevertheless examined by invoking anomalous fast ion diffusion from the plasma core. A significant $\chi_{\mathrm{fast}}(\sim 4\ \mathrm{m}^2/\mathrm{s})$ was needed to cause a change in the thermal diffusivities

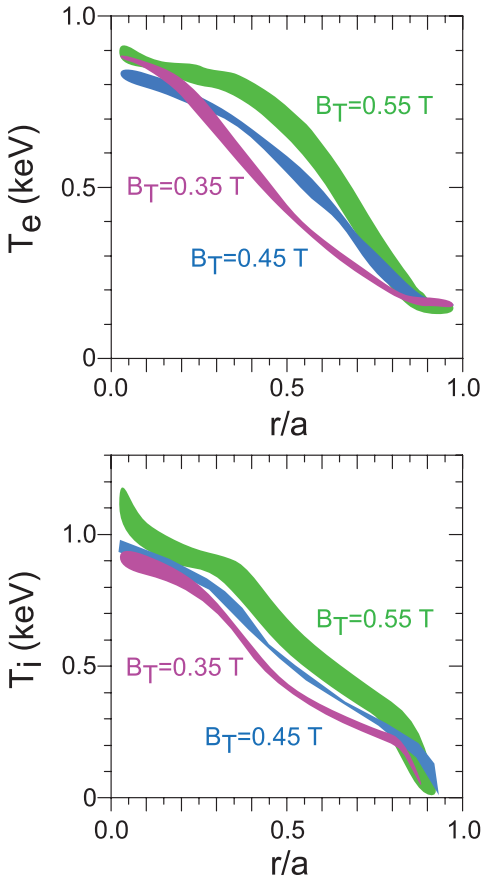

FIG. 2 (color). Electron (top) and ion (bottom) temperature profiles from the B_T scan at $I_p = 0.7$ MA. The band for each condition is the envelope of profiles for that condition.

outside their typical uncertainty of 20% to 30% in the region of $r/a \sim 0.65$ [10]. This would lead to a significant reduction in the calculated neutron signal and a large disagreement with the measured signal, which is due mostly to beam-target reactions. Consequently, based on the agreement in the calculated and measured neutrons in the base cases, and the uncertainties in the thermal diffusivities, the assumption of classical slowing down of beam ions is a reasonable one.

The electron and ion temperature profiles for the discharges in the B_T scan are shown in Fig. 2. The thickness of the line for each profile represents the envelope of profiles for that particular condition. The T_e profiles exhibit a marked broadening with increasing B_T, with the central electron temperature remaining approximately constant. The ion temperature profiles increase only marginally across the entire profile with increasing B_T.

The electron and ion thermal diffusivities are shown in Fig. 3. The electron thermal diffusivity, χ_e (top panel), varies the most as the toroidal field varies. The χ_e decreases significantly outside of $r/a = 0.5$ as B_T increases, reflecting the broadening of the electron temperature profiles. The χ_e profiles pivot at $r/a = 0.5$; inside of that radius the thermal diffusivities actually increase with increasing B_T, reflecting the increased flattening of the T_e profiles in this region. The increasing $\chi_e s$ in this low-volume region of the plasma has a minor effect on the overall confinement scaling. The ion thermal diffusivities (bottom panel) change very little with the variation in B_T, and the values are within the range of the neoclassical transport coefficients (brown hatched region) as computed by the GTC-NEO code, [11] which takes into account finite banana width, and thus nonlocal, effects. Also, outside of $r/a = 0.5$, it is seen that $\chi_i \geq \chi_e$ at the higher B_T. In these discharges, the ion-electron coupling term ranges from 10% to 25% of the electron thermal conduction loss near $r/a = 0.65$.

Temperature profiles from the I_p scan at $B_T = 0.55$ T are shown in Fig. 4. There is a 20% to 30% increase in the central electron temperature as I_p increases (top panel), mostly between 0.9 and 1.1 MA, and there is little change in the T_e outside of $r/a = 0.4$. On the other hand, the change in the T_i profile with plasma current is stronger (bottom panel), with a monotonic increase in central ion temperature of about 55% going from the lowest to highest current. The ion temperature profile shapes remain essentially the same for all currents; there is no marked broad-

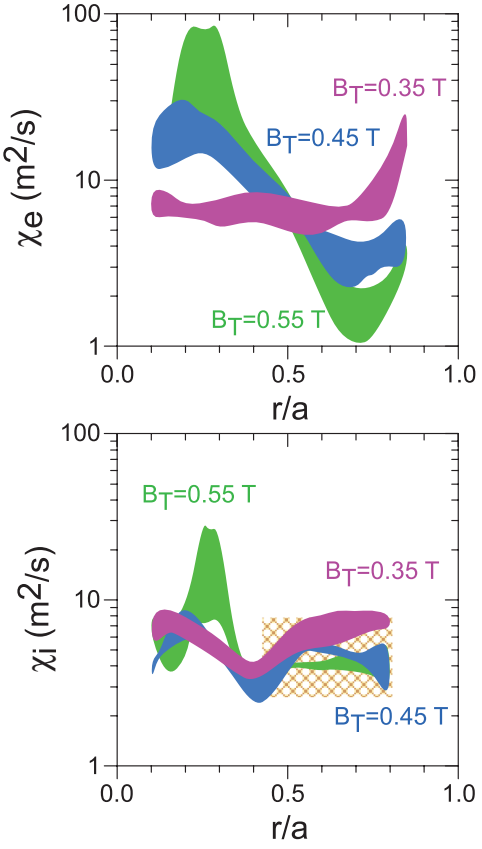

FIG. 3 (color). Electron (top) and ion (bottom) thermal diffusivities from the B_T scan at $I_p = 0.7$ MA. The brown cross hatched region outside $r/a = 0.5$ is the range of ion neoclassical thermal diffusivity as calculated by GTC-NEO.

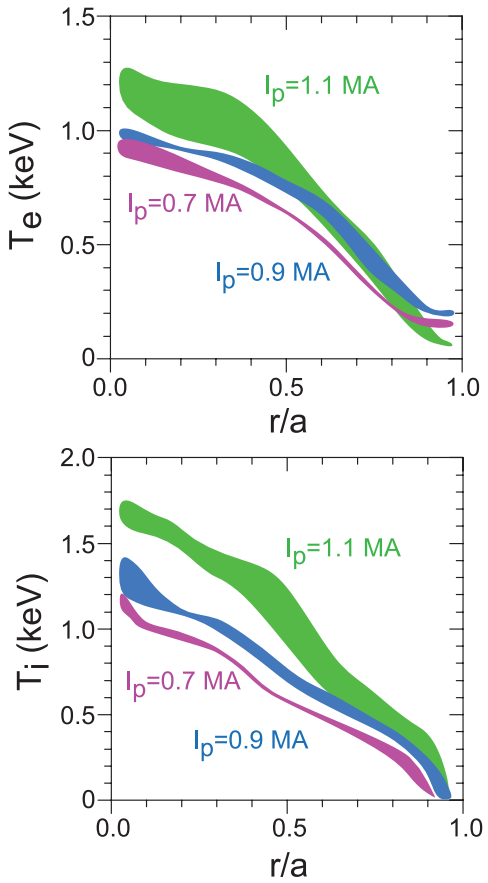

FIG. 4 (color). Electron (top) and ion (bottom) temperature profiles from the I_p scan at $B_T = 0.55$ T.

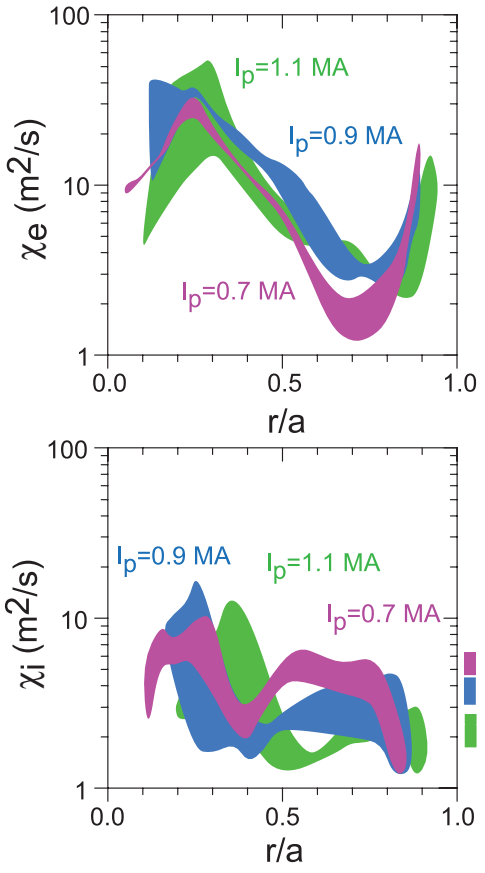

FIG. 5 (color). Electron (top) and ion (bottom) thermal diffusivities from the I_p scan at $B_T = 0.55$ T. The color-coded rectangles to the right of the graph are the neoclassical ranges computed by GTC-NEO for $r/a = 0.5$ to 0.8.

ening as was seen for the T_e profiles with increasing B_T (Fig. 2).

The electron and ion thermal diffusivities for the I_p scan are shown in Fig. 5. The χ_e changes only slightly as the plasma current is increased. The ion thermal diffusivity, however, decreases with increasing plasma current outside of $r/a = 0.4$, but changes very little inside that radius. Conversely with respect to the confinement trend with B_T where it is the electrons that control that scaling, it is the ions that are primarily responsible for the increase of confinement with I_p. Furthermore, the ion thermal diffusivities in the discharges from the I_p scan are also at the neoclassical level as determined by GTC-NEO. The levels of ion neoclassical χ_i in the region from $r/a = 0.5$ to 0.8 are indicated by the color-coded rectangles to the right of the bottom panel. As is seen, the range of χ_is inferred from the experimental measurements by TRANSP in the region of $r/a = 0.5$ to 0.8 is at the neoclassical level for each current, and it is the change of $\chi_{i,\mathrm{neo}}$ with plasma current that underlies the change in overall confinement with I_p. It is also seen that at the lowest current $\chi_i \geq \chi_e$.

In summary, for the first time, H-mode confinement trends from dedicated scans on a high-power spherical torus have been determined. Experiments on NSTX run at constant density and neutral beam heating power have successfully isolated the B_T and I_p dependences of both the thermal and global confinement time in lower single null H modes with small ELMs. The observed dependences differ from those observed at higher aspect ratio, with a stronger toroidal field dependence (nearly linear at a fixed current of 0.7 MA, and slightly weaker at 0.9 MA), and a weaker than linear dependence on plasma current.

While it is primarily a reduction in electron transport outside $r/a = 0.5$ with toroidal field that is responsible for the overall improvement of confinement with B_T, it is the change in ion thermal transport in this region, which is at the neoclassical level, that appears to control the I_p scaling. Also, while the electron thermal transport was always anomalous, $\chi_e \leq \chi_i$ at low current and high toroidal field (i.e., relatively higher q). Gyrokinetic and fluid calculations indicate that the short wavelength electron temperature gradient mode is a candidate for controlling the electron transport under certain conditions, most notably at low toroidal field [12]. Further experiments, making use of the newly implemented microwave scattering diagnostic to measure high-k turbulence NSTX, coupled to linear and nonlinear gyrokinetic analyses, will help identify the source(s) of the anomalous electron transport over a broader parameter range.

This work was supported by U. S. Department of Energy Contract No. DE-AC02-76CH03073 at the Princeton Plasma Physics Laboratory, and No. DE-FG02-99ER54524 at Columbia University. The authors would like to thank the entire NSTX operations, physics, and engineering teams for their contributions to this effort.

[1] S. M. Kaye *et al.*, Nucl. Fusion **45**, S168 (2005).
[2] J. E. Menard *et al.* Nucl. Fusion (to be published).
[3] G. Rewoldt *et al.*, Phys. Plasmas **3**, 1667 (1996).
[4] S. M. Kaye *et al.*, Nucl. Fusion **46**, 848 (2006).
[5] ITER Physics Basis, Nucl. Fusion **39**, 2137 (1999).
[6] R. Maingi *et al.*, Nucl. Fusion **45**, 264 (2005).
[7] J. E. Menard *et al.*, Phys. Rev. Lett. **97**, 095002 (2006).
[8] R. J. Hawryluk in *Physics of Plasmas Close to Thermonuclear Conditions* edited by B. Coppi, G. G. Leotta, D. Pfirsch, R. Pozzoli, and E. Sindoni (Pergoma, New York, 1980) (CEC, Brussels) Vol. 1, p. 19.
[9] R. J. Goldston *et al.*, J. Comput. Phys. **43**, 61 (1981).
[10] B. P. LeBlanc *et al.*, Nucl. Fusion **44**, 513 (2004).
[11] W. Wang *et al.*, Comput. Phys. Commun. **164**, 178 (2004).
[12] S. M. Kaye, Nucl. Fusion (to be published).